ACS OMEGA

http://pubs.acs.org/journal/acsodf

Article

Contribution of dsRBD2 to PKR Activation

Stephen Hesler, Matthew Angeliadis, Bushra Husain, and James L. Cole*

Cite This: *ACS Omega* 2021, 6, 11367−11374

Read Online

ACCESS | Metrics & More | Article Recommendations | Supporting Information

ABSTRACT: Protein kinase R (PKR) is a key pattern recognition receptor of the innate immune pathway. PKR is activated by double-stranded RNA (dsRNA) that is often produced during viral genome replication and transcription. PKR contains two tandem double-stranded RNA binding domains at the N-terminus, dsRBD1 and dsRBD2, and a C-terminal kinase domain. In the canonical model for activation, RNAs that bind multiple PKRs induce dimerization of the kinase domain that promotes an active conformation. However, there is evidence that dimerization of the kinase domain is not sufficient to mediate activation and PKR activation is modulated by the RNA-binding mode. dsRBD2 lacks most of the consensus RNA-binding residues, and it has been suggested to function as a modulator of PKR activation. Here, we demonstrate that dsRBD2 regulates PKR activation and identify the N-terminal helix as a critical region for modulating kinase activity. Mutations in dsRBD2 that have minor effects on overall dsRNA-binding affinity strongly inhibit the activation of PKR by dsRNA. These mutations also inhibit RNA-independent PKR activation. These data support a model where dsRBD2 has evolved to function as a regulator of the kinase.

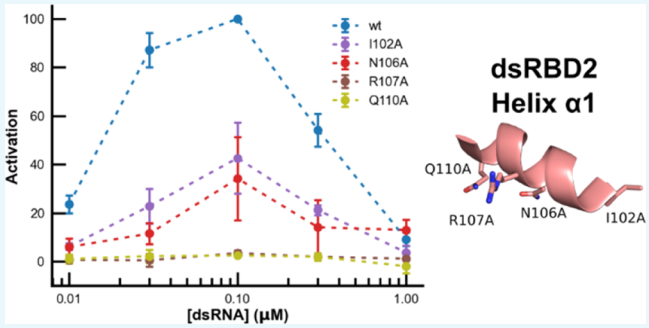

INTRODUCTION

Protein kinase R (PKR) is a key mediator in the innate immune response to viral infection.[1] PKR is activated by dsRNAs or RNAs containing duplex regions produced during viral genome replication and viral mRNA transcription.[2,3] Upon binding activating RNAs, PKR undergoes autophosphorylation, inducing a transition to an active kinase. Activated PKR phosphorylates the eukaryotic initiation factor eIF2α, disrupting *de novo* protein synthesis and blocking viral replication.

PKR contains three independently folding domains: two N-terminal tandem class A double-stranded RNA-binding domains[4,5] [dsRBD1 and dsRBD2, together referred to as the regulatory domain (RD)] and a C-terminal kinase domain (KD).[6] The RD and KD are tethered *via* a ∼90 amino acid flexible unstructured linker. The KD adopts a canonical bilobal Ser/Thr kinase fold with a rotated helix αG in the C-lobe associated with the recognition of eIF2α.[6] The KD crystallizes as a parallel, back-to-back dimer with the active sites facing away from the dimer interface.[6−8] In the NMR structure of the RD, each dsRBD has the canonical α-β-β-β-α fold.[5] In contrast to dsRBD1, dsRBD2 lacks many of the consensus RNA-binding residues and it has little or no affinity for RNA on its own.[9] However, the presence of dsRBD2 enhances the affinity relative to dsRBD1 alone.[10]

Structural, biochemical, and biophysical analyses support a pivotal role for dimerization in the activation of PKR.[11] Disruption of salt bridges across the PKR dimer interface blocks activation.[12] PKR forms a weak (K_d ∼ 0.5 mM) dimer in solution and dimerization of PKR at a high concentration induces activation in the absence of RNA.[13] In the context of simple RNA duplexes, a minimum of 30 bp of dsRNA are required to bind two PKRs and to activate autophosphorylation, supporting a minimal model where the role of the dsRNA is to bring two or more PKR monomers in close proximity to enhance dimerization.[14]

There is evidence that PKR activation is modulated by the RNA-binding mode. We have identified several RNAs that can bind two PKR monomers and induce kinase domain dimerization but nonetheless fail to activate.[15,16] Affinity cleavage measurements suggested that simultaneous binding of both dsRBDs occurs only on activating RNAs.[17] NMR data indicate that only the N-terminus of dsRBD2 interacts with a short, nonactivating dsRNA, but extensive interactions with dsRBD2 occur upon binding to a longer, activating sequence.[10] Other NMR chemical shift perturbation studies demonstrate that dsRBD2 weakly interacts with the KD.[18,19] Taken together, these results imply that the dsRBD2 functions to regulate the activity of the KD by direct interaction.

Here, we have introduced mutations into dsRBD2 intended to disrupt dsRBD2−dsRNA interactions to probe the

Received: January 19, 2021
Accepted: April 2, 2021
Published: April 19, 2021

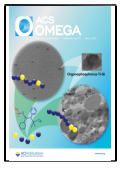

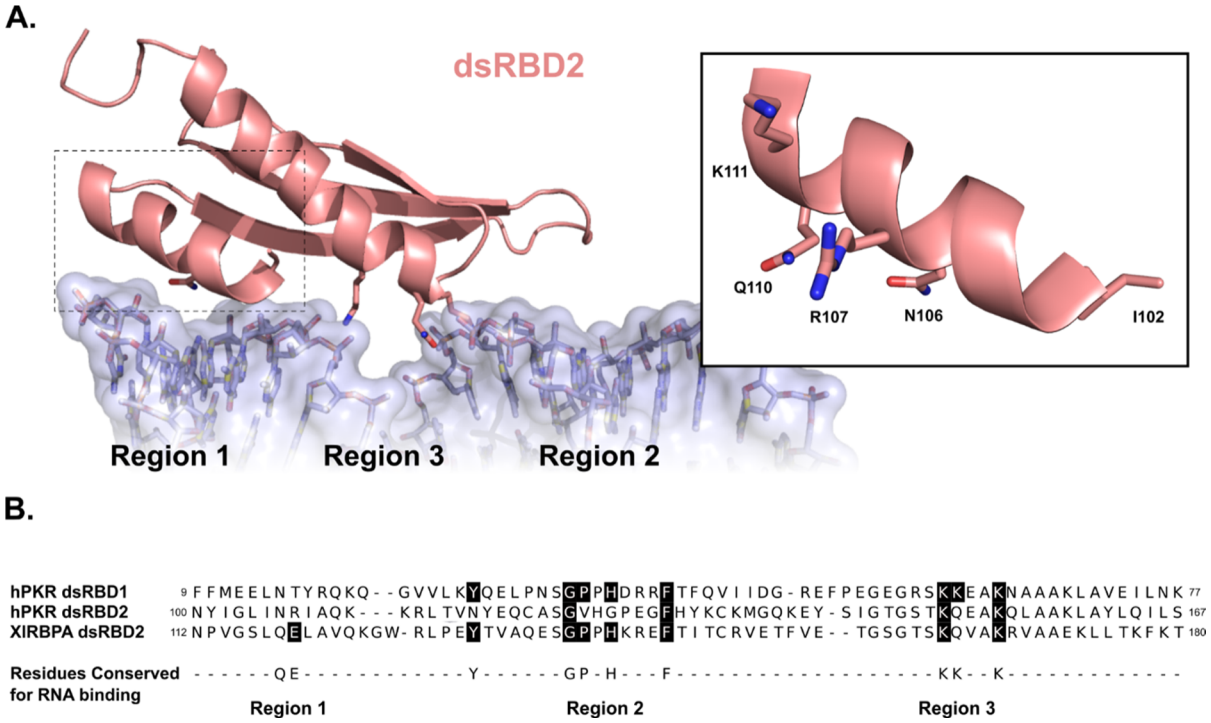

Figure 1. Identification of putative RNA-binding residues in dsRBD2. (A) Model of PKR dsRBD2 bound to dsRNA. Model was created by the structural alignment of PKR dsRBD2 (PDB: 1QU6) with an xlrbpa2/dsRNA complex (PDB: 1DI2). Side chains of putative RNA contacting residues in regions 1, 2, and 3 are depicted as sticks. Inlay shows a close-up view of helix α1 with surface-exposed side chains shown. (B) Sequence alignment of PKR dsRBD1, dsRBD2, and xlrbpa dsRBD2. The consensus dsRBD RNA-binding residues in regions 1, 2, and 3 are shown below. Residues that match the consensus are highlighted.

contribution of dsRBD2 to PKR activation. Surprisingly, we identified key mutations on dsRBD2 that have minor effects on overall dsRNA-binding affinity while strongly inhibiting the activation of PKR by dsRNA. These mutations also inhibit RNA-independent PKR activation. These data support a model where dsRBD2 has evolved to function as a regulator of the kinase.

RESULTS

Identification of Candidate RNA-Binding Residues in PKR dsRBD2. In order to determine which residues in PKR dsRBD2 are likely to directly contact RNA, we created a model of the PKR dsRBD2−dsRNA complex based on a structural alignment with the dsRNA complex of the second dsRBD of *Xenopus laevis* RNA-binding protein A (xlrbpa2) (Figure 1A).[20] Typically, dsRBDs contact one face of the dsRNA and interact with two sequential minor grooves and the intervening major groove in regions 1, 2, and 3, respectively. Region 1 corresponds to helix α1, region 2 is the loop between strands β1 and β2, and region 3 encompasses the N-terminus of helix α2. In this model, regions 1 and 3 are positioned to interact with the dsRNA, but region 2 is displaced from the RNA. This loop may be able to reorient to contact the nearby minor groove. The residues that are typically conserved for RNA binding in these regions are depicted in a sequence alignment (Figure 1B). PKR dsRBD2 differs from the consensus in all three regions, but residues in region 3 are more conserved. K150 and K154 on dsRBD2 both align well with conserved region 3 lysines. Mutation of either K150 or K154 blocks RNA binding by PKR.[21] A third lysine is absent, replaced by Q151, which appears capable of interacting within the RNA major groove. Residues in region 2 lie in the flexible loop between β-strands 1 and 2 and are difficult to predict due to the variability in loop length and flexibility. In region 1, *Q* is replaced by a conservative substitution (N106) and *E* is replaced by R107. N106 appears positioned to interact with RNA. Based on these observations, we created a PKR mutant containing alanine substitutions in all three regions: N106A/H126A/K150A/Q151A (NHKQ). Figure 2 shows a titration of PKR autophosphorylation induced by a 40 bp dsRNA. Wild-type PKR exhibits the classical bell-shaped activation curve where concentrations of RNA above 0.1 μM inhibit due to the

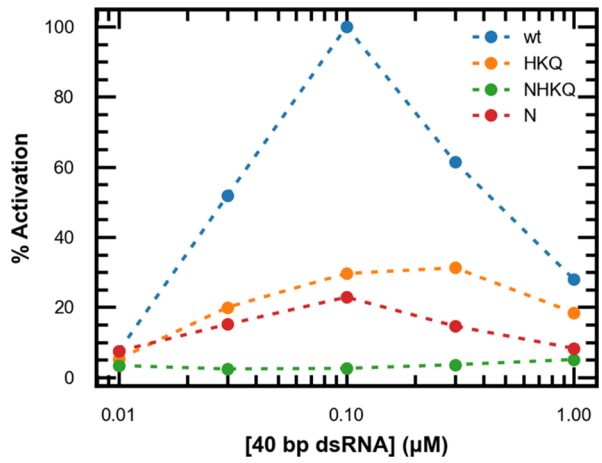

Figure 2. Effect of dsRBD2 mutations on the activation of PKR by 40 bp dsRNA. Constructs "N" and "HKQ" contain mutations in regions 1 and 2 + 3, respectively. Construct "NHKQ" contains mutations in all three regions. Data are normalized to the activation of wild-type PKR at 0.1 μM 40 bp dsRNA.

https://doi.org/10.1021/acsomega.1c00343
ACS Omega 2021, 6, 11367−11374

Table 1. Effect of Helix α1 Mutations on PKR−RNA Binding Affinities[a]

mutant	K_{d1} (μM)	K_{d2} (μM)	RMSD[b]	max RP_2[c]
WT	0.166 (0.089, 0.321)	0.487 (0.406, 0.578)	0.0123	0.149
I102A	0.184 (0.104, 0.320)	0.703 (0.593, 0.834)	0.0123	0.112
N106A	0.231 (0.212, 0.252)	0.847 (0.823, 0.871)	0.0076	0.096
R107A	0.225 (0.144, 0.335)	1.103 (0.930, 1.328)	0.0095	0.077
Q110A	0.245 (0.152, 0.376)	1.135 (0.953, 1.379)	0.0103	0.075
K111A	0.399[d]	0.564[d]	0.0117	0.133

[a]Parameters obtained by global nonlinear least-square analysis of the sedimentation velocity data using a model of sequential binding of two protein monomers. The values in parentheses represent the 95% joint confidence intervals obtained using the F-statistic. [b]Root-mean-square deviation in absorbance units. [c]The maximum fractional concentration of the active species containing two PKRs bound to a single RNA at [PKR] = 200 nM. [d]Confidence intervals could not be obtained.

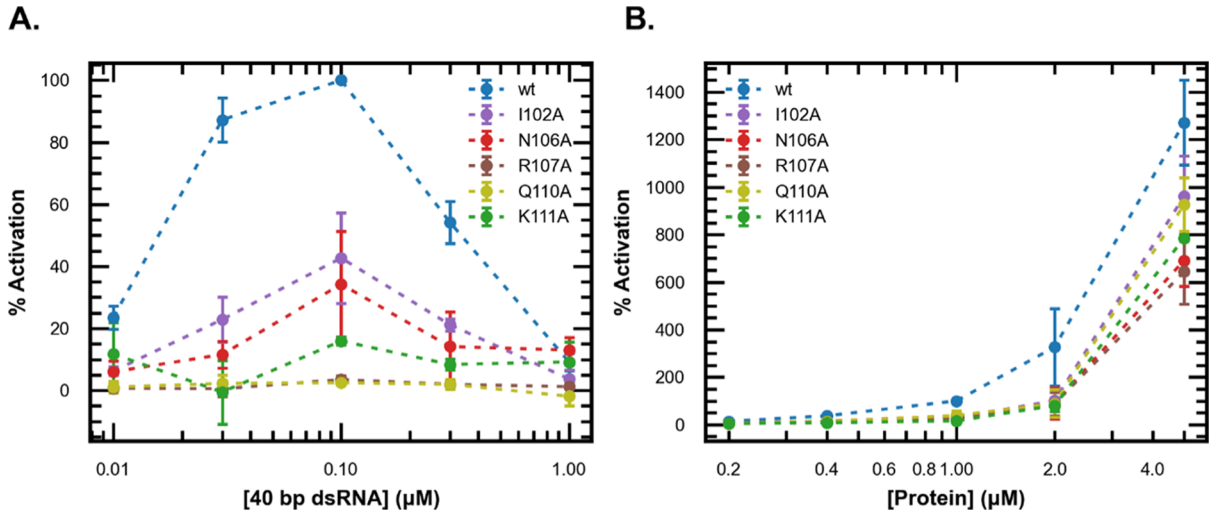

Figure 3. Effect of dsRBD2 helix α1 mutations on PKR activation. (A) Analysis of PKR activation by 40 bp dsRNA. The data are normalized to wild-type PKR activation at 0.1 μM 40 bp dsRNA. (B) Analysis of PKR autoactivation. The data are normalized to wild-type PKR at 1 μM.

dilution of PKR onto separate molecules of RNA. The NHKQ mutant is completely inactive in this assay. Partial activation is retained upon restoring N106 in H126A/K150A/Q151A (HKQ). Conversely, the N106A (N) mutation alone results in substantial inhibition. These results indicate that the disruption of dsRBD2−RNA interactions blocks PKR activation and points toward region 1 as particularly important in modulating kinase activity. For this reason, we focused on this region of dsRBD2 in further mutagenesis studies.

Analysis of RNA-Binding Affinities. In addition to the consensus RNA-binding residues in region 1 (QE, Figure 1B), dsRBDs often make additional interactions with RNA using surfaced-exposed residues lying within helix α1.[22] These interactions are not conserved and are believed to confer a degree of sequence specificity to some dsRBDs.[22,23] These positions correspond to I102, G103, N106, R107, and Q110 in PKR dsRBD2 (Figure 1A). In order to define the contribution of dsRBD2 helix α1 to RNA binding and PKR activation, we introduced alanine substitution at each of these positions and measured binding to these mutants to an activating 40 bp dsRNA (Figure S4) by sedimentation velocity analytical ultracentrifugation. Under the conditions of this experiment (200 mM NaCl), this RNA binds two PKR monomers,[24] and the data obtained at multiple protein concentrations were globally fit to a simple sequential binding model

$$2P + R \overset{K_{d1}}{\longleftrightarrow} P + RP \overset{K_{d2}}{\longleftrightarrow} RP_2 \quad (1)$$

where P is PKR, R is RNA, and K_{d1} and K_{d2} are the dissociation constants for binding the first and second PKR, respectively.

An example global fit is shown in Figure S1, and the results are given in Table 1. Each helix α1 mutation weakens binding affinity, causing increases in the dissociation constants for the first (K_{d1}) and second (K_{d2}) PKR. In order to interpret these data in the context of their effects of PKR kinase activity, we modeled the distribution of PKR species based on these binding parameters. In the dimerization model for the activation of PKR, the active species is RP_2, a dsRNA containing two bound PKRs. We calculated the maximal fractional concentration of RP_2 for wild-type PKR and each of the mutants (Table 1). The R107A and Q110A mutants exhibit the largest decrease in maximal RP_2 to about 50% of the wild type. The maximal RP_2 for the K111A construct is similar to the wild type, while the I102A and N106A mutants fall in between. Thus, these mutants only modestly decrease the affinity of PKR for an activating RNA.

Effect of Helix α1 Mutations on PKR Activation. The dsRBD2 helix 1 mutants were assayed for kinase activation by the 40 bp dsRNA by measuring autophosphorylation (Figure 3A). Unlike the relatively weak effects on RNA binding induced by helix α1 point mutations, they profoundly reduce the maximal extent of PKR activation. Two mutants, R107A and Q110A, are completely inactive in this assay despite retaining half of the maximal RP_2 amplitude of wild-type RNA. I102A and N106A PKR exhibit about 40% of wild-type

https://doi.org/10.1021/acsomega.1c00343
ACS Omega 2021, 6, 11367−11374

activity. Interestingly, activation of K111A decreased to ∼15% of wild-type PKR despite retaining near wild-type dsRNA affinity. The much greater effects of helix α1 mutations on PKR activation by dsRNA compared to RNA-binding affinity suggest that this helix must participate in an essential interaction required for PKR activation.

In order to further probe the contribution of helix α1 on PKR activation, we carried out PKR activation assays on the surface mutants in the absence of RNA. Dimerization of PKR at higher protein concentrations above 0.5 μM induces autophosphorylation in the absence of RNA.[13] Figure 3B shows that wild-type PKR undergoes RNA-independent activation upon increasing the protein concentration from 0.4 to 1 μM and the extent of autophosphorylation strongly increases at higher concentrations. Interestingly, all of the mutants are essentially inactive in this assay at 1 μM. At higher protein concentrations, the PKR mutants undergo autophosphorylation, but the extent of activation is reduced relative to the wild type. These data demonstrate that helix α1 in dsRBD2 plays a role in PKR activation independently of its contribution to RNA-binding affinity. It is noteworthy that all of the mutants can undergo RNA-independent autophosphorylation at the highest protein concentrations, demonstrating that their catalytic activity is impaired but not completely blocked. We confirmed this observation in the context of RNA-dependent activation of PKR using a more potent activating RNA (Figure S3). Although PKR R107A does not display measurable activation by 40 bp dsRNA, it undergoes activation induced by high concentrations of poly(rI)·poly(rC). As in the case of RNA-independent activation, this mutant is much less active than wild-type PKR.

Effect of Helix α1 Mutations on KD Dimerization. The dsRBD2 helix α1 surface mutants retain the ability to form RP_2 complexes with only minor reduction in RNA-binding affinity, suggesting that a subsequent step in the activation process is inhibited. A potential mechanism is the disruption of KD dimerization. We developed a sensitive homo-FRET assay to directly monitor the dimerization of the KD upon RNA binding.[15] This assay monitors depolarization of fluorescence emission from Alexa Fluor 488-labeled PKR due to homo-FRET that accompanies formation of the KD dimer.

Titration of wild-type PKR with 40 bp dsRNA induces a decrease in fluorescence anisotropy that is reversed at higher RNA concentrations due to a dilution of the labeled PKR onto separate dsRNA molecules (Figure 4). PKR N106A and Q110A each show a decrease in anisotropy similar to wild-type PKR, indicating that these mutations do not affect the ability to form KD dimers upon the formation of RP_2. Given that the maximal fraction of the RP_2 species formed by Q110A is about one-half of the wild type (Table 1), it is surprising that the anisotropy change for this mutant is not similarly reduced. In contrast, R107A exhibits an attenuated anisotropy change that correlates with the reduced concentration of RP_2. These data demonstrate that N106A and Q110A undergo KD dimerization upon binding to an activating RNA but dimerization is impeded in R107A PKR. Thus, the reduced activity of N106A and Q110A PKR cannot be ascribed to a defect in KD dimerization, but such a defect may contribute to the absence of kinase activity of R107A PKR stimulated by 40 bp dsRNA.

Sedimentation equilibrium experiments were employed to determine the origin of the reduced RNA-dependent KD dimerization of the R107A mutant by probing dimerization in the absence of RNA. This assay directly measures the overall

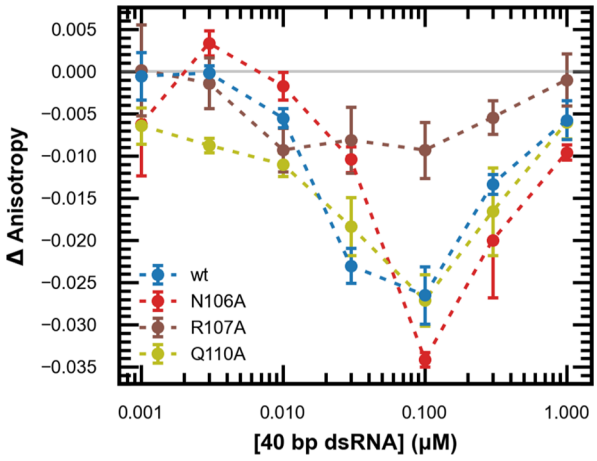

Figure 4. Effect of dsRBD2 helix α1 mutations on PKR dimerization. KD dimerization was assayed by homo-FRET-induced depolarization of fluorescence emission. PKR constructs were labeled with Alex Fluor 488 at position 261 on the kinase domain using unnatural amino acid mutagenesis as described in Materials and Methods. The protein concentration was held constant at 0.2 μM with the increasing concentration of 40 bp dsRNA. The anisotropy of the free protein was subtracted.

affinity for protomer dimerization. As we previously reported,[13] wild-type PKR dimerizes weakly, with K_d = 702 (560, 921) μM (values in parenthesis represent the 95% confidence intervals). R107A PKR dimerizes with similar affinity [K_d = 704 (638, 778) μM], demonstrating that the reduced RNA-dependent dimerization is not reflected in the behavior of the RNA-free enzyme. These results also show that the impaired RNA-independent activity of the dsRBD2 helix α1 mutants is not due to a dimerization defect but instead reflects the disruption of regulatory interactions between dsRBD2 and the kinase domain.

Analysis of dsRBD2−RNA Interactions. The sedimentation velocity analysis of PKR−RNA interactions demonstrates that the dsRBD2 helix α1 mutations only modestly affect the binding affinity. However, this method only monitors the overall binding of the protein to the RNA. Potentially, these mutations disrupt the binding of dsRBD2 to RNA without strongly affecting the overall affinity. To test this hypothesis, we developed a tryptophan fluorescence anisotropy assay to independently monitor dsRBD1 and dsRBD2 binding to dsRNA. We utilized a PKR RD construct containing dsRBD1 and dsRBD2 that contains no native tryptophans. It is known from NMR measurements that the two dsRBDs in the RD tumble independently in solution.[5,19] Single tryptophans were selectively introduced into either dsRBD1 or dsRBD2 to produce domain-specific probes of rotational mobility. Two mutations, F131W and Y142W, are located on strands β_2 and β_3, respectively, on dsRBD2, removed from the putative dsRNA-binding surface. The analogous mutation to F131W on dsRBD1, F41W, was created as a control.

This assay was validated using 20 and 40 bp dsRNAs. Our previous NMR analysis showed that dsRBD1 engages both RNAs equivalently. In contrast, only the N-terminal region of dsRBD2 engages with the shorter RNA, but more extended interactions occur with the longer 40 bp RNA.[10] The anisotropy experiments were performed under near-stoichiometric binding conditions where [RD] > K_d. When F41W PKR is titrated with 40 bp dsRNA, there is an increase in anisotropy

https://doi.org/10.1021/acsomega.1c00343
ACS Omega 2021, 6, 11367−11374

plateauing near 0.5 μM RNA (Figure 5, blue). This behavior is consistent with the expected 2:1 binding stoichiometry at a

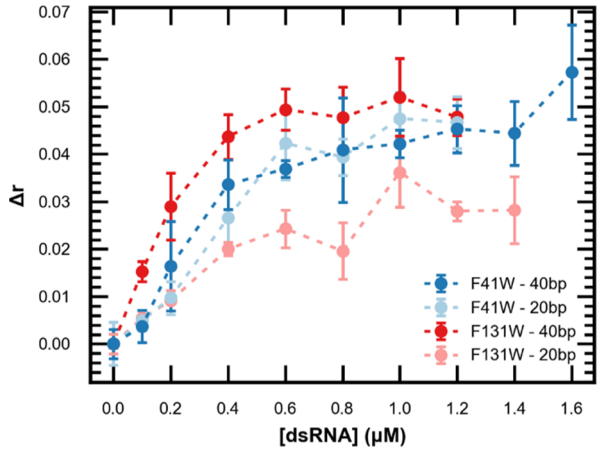

Figure 5. Analysis of dsRBD1/2 tryptophan anisotropy changes upon binding 40 bp and 20 bp dsRNAs. Blue lines identify mutation F41W to monitor dsRBD1 binding to 40 bp (dark blue) or 20 bp (light blue) dsRNAs. Red lines identify mutation F131W to monitor dsRBD2 binding 40 bp (dark red) or 20 bp (light red) dsRNAs. The anisotropy in the absence of RNA was subtracted. The protein concentration was 1 μM with increasing dsRNA concentration up to 1.6 μM.

protein concentration of 1 μM. The fact that the anisotropies plateau indicates that the rotational mobility of dsRBD1 is not strongly affected by the dilution of the RD onto separate RNAs. Repeating the assay with 20 bp dsRNA yields a virtually identical stoichiometric increase in anisotropy (Figure 5, light blue), demonstrating that dsRBD1 interacts similarly with the two RNAs. In contrast, experiments with F131W to monitor dsRBD2 binding show a significantly greater increase in anisotropy when titrated with 40 bp dsRNA as compared to 20 bp dsRNA (Figure 5, red and light red, respectively). These data are consistent with our previous NMR results[10] in demonstrating that dsRBD1 interacts equivalently with the short and long dsRNAs, but the rotational motion of dsRBD2 is less restrained upon binding to the shorter RNA.

The two mutations that most inhibited PKR activation by 40 bp dsRNA (R107A and Q110A) were introduced into the F41W, F131W, and Y142W constructs to assess the effect of dsRBD2 helix α1 mutations on the engagement of the individual dsRBDs. Each of these constructs was titrated with 40 bp dsRNA. As expected for the F41W constructs that monitor dsRBD1 rotational mobility, the introduction of R107A and Q110A mutations on dsRBD2 helix α1 does not significantly affect the RNA-induced anisotropy changes (Figure 6A). Interestingly, when the tryptophan is located in dsRBD2 at positions F131W (Figure 6B) or Y142W (Figure 6C) in dsRBD2, the R107A and Q110A mutations also do not attenuate the anisotropy increases. Thus, the loss of kinase activation associated with these mutations in dsRBD2 helix α1 is not associated with a detectable change in the mode of binding of dsRBD2 with dsRNA.

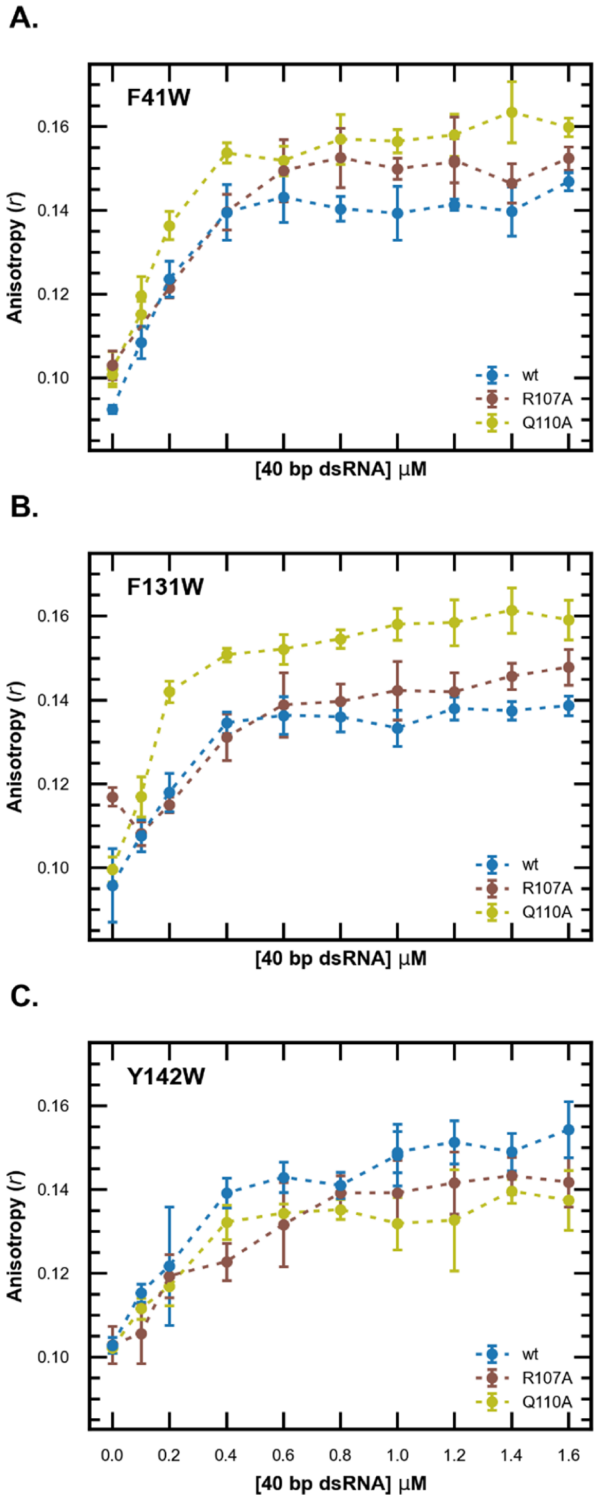

Figure 6. Effect of dsRBD2 helix α1 mutations on tryptophan anisotropy changes induced by RNA-binding wild type (blue), R107A (brown), and Q110A (yellow). A single tryptophan was introduced into dsRBD1 at position F41 (A) or into dsRBD2 at positions F131 (B) and Y142 (C). The anisotropy in the absence of RNA was subtracted. The protein concentration was 1 μM with increasing dsRNA concentration up to 1.6 μM.

DISCUSSION

In order to define the role of dsRBD2 in mediating PKR activation, we introduced mutations in this domain intended to disrupt RNA binding. As expected, mutating key residues in all three RNA-binding regions of dsRBD2 completely inhibits RNA-induced autophosphorylation. In the course of these studies, we discovered that the N-terminal helix (α1) of dsRBD2 functions as a regulator of the kinase activity of PKR

https://doi.org/10.1021/acsomega.1c00343
ACS Omega 2021, 6, 11367−11374

independent of its RNA-binding function. Mutations in this region inhibit dsRNA-induced PKR activation while only modestly affecting overall dsRNA-binding affinity. Our results agree with previous studies demonstrating that the mutation of PKR Q110 in dsRBD2 reduces RNA binding with only minor effects on PKR dimerization.[21] For two of these mutants that show no RNA-induced activation, domain-resolved fluorescence anisotropy experiments show that dsRBD2 can engage with dsRNA. Remarkably, the helix α1 mutations also inhibit RNA-independent activation of PKR mediated by dimerization at high protein concentrations. This inhibition is not due to a global disruption of protein folding or conformation as the sedimentation coefficients of the mutant PKR constructs are very close to the wild type (Figure S2).

We propose that the regulation of PKR activity by dsRBD2 is mediated by direct interaction with the KD. Previous biophysical data demonstrate such an interaction. Addition of a dsRBD construct induces NMR chemical shift perturbation in KD resonances,[18] and conversely, addition of KD induces chemical shift perturbation in dsRBD2.[19] Sedimentation velocity experiments detect the interaction of RD and KD constructs with $K_d \sim 250$ μM.[25] Although this affinity is quite low, these domains are tethered together by an unstructured linker that favors the formation of an intramolecular interaction in the context of the holoenzyme. SAXS analysis demonstrates that PKR populates both open and closed conformations.[26] The stability of the KD is enhanced by ~1.5 kcal/mol in the context of the holoenzyme,[25] supporting the formation of interdomain interactions. PKR dsRBD2 lacks several of the consensus RNA-binding residues typically found in class A dsRBDs. There is precedent for atypical dsRBDs functioning as intramolecular or intermolecular protein−protein interaction motifs.[27]

An autoinhibition model for PKR activation has been proposed where the interaction of dsRBD2 with the KD sterically occludes the active site and locks the enzyme in an inactive, closed conformation.[2] RNA binding by dsRBD2 then releases this interaction, leading to kinase activation. Although the evidence cited above indicates that dsRBD2 interacts with the KD, this interaction does not impede the binding of the substrate ATP to the KD active site.[28] More recent structural and biophysical data favor a dimerization activation model whereby dsRNA binding tethers PKR monomers in close proximity and functions to induce dimerization of PKR *via* the KD.[11] In the context of the autoinhibition model, mutations in dsRBD2 that disrupt interaction with the KD would be expected to lead to constitutive PKR activation, which is not observed. Instead, the dsRBD2 mutations inhibit activation, indicating that dsRBD2 functions as a positive regulator of PKR activity where the interaction of dsRBD2 with the KD enhances catalytic activity. Thus, we propose that PKR activation requires both KD dimerization and interaction with dsRBD2. There is precedent for a dsRBD domain acting as a positive regulator. The protein activator of PKR, PACT, contains three dsRBDs.[29,30] While dsRBD1 and dsRBD2 of PACT bind dsRNA, dsRBD3 lacks conserved lysines in region 3 and does not interact with RNA. Instead, this third domain functions to activate PKR by binding to a loop in the N-lobe of the KD.[31] Interestingly, PKR dsRBD2 also binds to a peptide corresponding to the same N-lobe loop.

Dimerization is a key step in the activation of PKR, and it is noteworthy that RNA-dependent KD dimerization is retained in the N106A and Q110A mutants. This same phenotype is displayed upon binding of PKR to duplex RNAs containing 10−15 bp 2′-*O*-methyl barriers that induce KD dimerization but fail to activate.[15] Similarly, adenovirus VAI RNA produces KD dimers but does not activate PKR.[16] Finally, inactivating mutations within the PKR dimer interface that disrupt key electrostatic and hydrogen-binding interactions fail to abolish KD dimerization.[15] Together, these observations demonstrate that dimerization is a necessary but not sufficient step for the activation of PKR and point to the existence of one or more inactive dimer configurations. In addition to the back-to-back dimer interface that is associated with activation,[12] PKR can form a face-to-face interface that mediates trans-autophosphorylation within the activation loop.[8] Another eIF2α kinase, GCN2, can adopt an active parallel back-to-back KD structure[32] as well as an inactive, antiparallel back-to-back dimer configuration.[33] Interaction of dsRBD2 with the KD may modulate the nature of the PKR dimer formed and thus regulate catalytic activity to provide a mechanism for distinguishing between host and pathogen RNA.

MATERIALS AND METHODS

Reagents. All buffers were prepared using reagent-grade chemicals and sterile filtered prior to use. Unphosphorylated human PKR[14,34] (Uniprot accession ID: P19525) and PKR RD (residues 1−185)[35] were expressed in *E. coli* and purified as previously described. In the final purification step, PKR and PKR RD were subject to gel filtration in the AU200 buffer (20 mM HEPES, 200 mM NaCl, 0.1 mM EDTA, 0.1 mM TCEP, pH 7.5). Mutant constructs were generated by QuikChange site-directed mutagenesis of the parental plasmid using oligonucleotide primers containing the desired mutations.

Sedimentation velocity analytical ultracentrifugation of wild-type PKR and the dsRBD2 helix α1 mutants demonstrate that all of these constructs are all well folded and exist predominantly as monomers (s = 3.3−3.4 S) with a minor (1−4%) dimer contaminant at 5.60 S (Figure S2). PKR was labeled with Alexa Fluor 488 at position 261 by unnatural amino acid mutagenesis as previously described.[15] RNAs were purchased from Horizon Discovery, deprotected according to the manufacturer's protocol, and purified by denaturing (8 M urea) gel electrophoresis. Complementary single stranded RNAs were annealed by heating to 80 °C and slowly cooling to room temperature. RNA sequences can be found in Figure S4.

Activation Assays. PKR autophosphorylation activity was measured by quantifying ^{32}P incorporation from [γ-^{32}P]ATP (PerkinElmer). Reactions were performed using 200 nM PKR in the AU200 buffer supplemented with 5 mM $MgCl_2$ at 32 °C for 20 min. ^{32}P incorporation was determined as previously described.[13,36]

Analytical Ultracentrifugation. RNA-binding affinities were measured using sedimentation velocity analytical ultracentrifugation as previously described.[37] Samples containing 0.4 μM 40 bp dsRNA and multiple PKR concentrations were prepared in the AU200 buffer, and data were collected at 40,000 rpm and 20 °C. Global data analysis using a 2:1 binding model was performed using SEDANAL.[38] Sedimentation equilibrium analysis of PKR dimerization was performed as previously described[13] over a protein concentration range of 0.25 to 1.5 mg/mL at 15,000, 18,000, and 22,000 rpm at 20 °C. SEDNTERP[39] was used to calculate buffer density, buffer viscosity, and protein partial specific volumes.

Fluorescence Anisotropy. Steady-state fluorescence measurements were taken using a Horiba Fluoromax-3

https://doi.org/10.1021/acsomega.1c00343
ACS Omega 2021, 6, 11367−11374

fluorimeter equipped with Glan-Thompson polarizers (Jobin Yvon Inc.). Fluorescence measurements were performed at 20 °C using 2 mm × 10 mm quartz cuvettes (Precision Cells). Kinase domain dimerization measurements were performed by measuring HOMO-FRET-mediated depolarization with PKR labeled at position 261 with Alexa Fluor 488 as previously described.[15] Tryptophan emission anisotropy was used to locally monitor the binding of dsRBD1 and dsRBD2 to RNA in the context of the PKR RD construct. The RD lacks any endogenous tryptophans residues, and single tryptophan substitutions were introduced into dsRBD1 and dsRBD2 on surface-exposed aromatic residues distal from the dsRNA-binding interface. dsRBD1 was labeled by F41W or F52W mutations, and dsRBD2 was labeled with the corresponding F131W or Y142W mutations. The RD F52W construct did not express well and was not used. Data were collected using excitation and emission wavelengths of 295 and 350 nm with 5 and 10 nm bandpasses, respectively. A minimum of three 5 s acquisitions were averaged to obtain standard errors less than 0.1%. Anisotropy, r, was calculated using the following equation

$$r = \frac{I_{\parallel} - GI_{\perp}}{I_{\parallel} + 2GI_{\perp}}$$

where $I_{\parallel}$ and $I_{\perp}$ correspond to parallel and perpendicular emission intensities, respectively, and G is the grating correction factor.

■ ASSOCIATED CONTENT

Supporting Information

The Supporting Information is available free of charge at https://pubs.acs.org/doi/10.1021/acsomega.1c00343.

Global analysis of PKR N106A binding to dsRNA, sedimentation velocity analysis of PKR constructs, activation of PKR R107A by poly(rI)·poly (rC), and RNA sequences (PDF)

■ AUTHOR INFORMATION

Corresponding Author

James L. Cole − *Department of Molecular and Cell Biology, University of Connecticut, Storrs 06269, Connecticut, United States; Department of Chemistry, University of Connecticut, Storrs 06269, Connecticut, United States;* orcid.org/0000-0002-9028-8364; Email: james.cole@uconn.edu

Authors

Stephen Hesler − *Department of Molecular and Cell Biology, University of Connecticut, Storrs 06269, Connecticut, United States*

Matthew Angeliadis − *Department of Molecular and Cell Biology, University of Connecticut, Storrs 06269, Connecticut, United States*

Bushra Husain − *Department of Molecular and Cell Biology, University of Connecticut, Storrs 06269, Connecticut, United States*

Complete contact information is available at: https://pubs.acs.org/10.1021/acsomega.1c00343

Funding

This work was supported by grant number AI-53615 from the NIH to J.L.C.

Notes

The authors declare no competing financial interest.

Accession Codes PKR P19525.1.

■ REFERENCES

(1) Williams, B. R. G. Signal integration via PKR. *Sci. Signal.* **2001**, *2001*, re2.

(2) Robertson, H. D.; Mathews, M. B. The regulation of the protein kinase PKR by RNA. *Biochimie* **1996**, *78*, 909−914.

(3) Clemens, M. J.; Elia, A. The double-stranded RNA-dependent protein kinase PKR: Structure and function. *J. Interferon Cytokine Res.* **1997**, *17*, 503−524.

(4) Patel, R. C.; Sen, G. C. Identification of the double-stranded RNA-binding domain of the human interferon-inducible protein kinase. *J. Biol. Chem.* **1992**, *267*, 7671−7676.

(5) Nanduri, S.; Carpick, B. W.; Yang, Y.; Williams, B. R. G.; Qin, J. Structure of the double-stranded RNA-binding domain of the protein kinase PKR reveals the molecular basis of its dsRNA-mediated activation. *EMBO J.* **1998**, *17*, 5458−5465.

(6) Dar, A. C.; Dever, T. E.; Sicheri, F. Higher-order substrate recognition of eIF2α by the RNA-dependent protein kinase PKR. *Cell* **2005**, *122*, 887−900.

(7) Li, F.; Li, S.; Wang, Z.; Shen, Y.; Zhang, T.; Yang, X. Structure of the kinase domain of human RNA-dependent protein kinase with K296R mutation reveals a face-to-face dimer. *Chin. Sci. Bull.* **2012**, *58*, 998−1002.

(8) Mayo, C. B.; Erlandsen, H.; Mouser, D. J.; Feinstein, A. G.; Robinson, V. L.; May, E. R.; Cole, J. L. Structural Basis of Protein Kinase R Autophosphorylation. *Biochemistry* **2019**, *58*, 2967−2977.

(9) Tian, B.; Mathews, M. B. Functional Characterization of and Cooperation between the Double-stranded RNA-binding Motifs of the Protein Kinase PKR. *J. Biol. Chem.* **2001**, *276*, 9936−9944.

(10) Ucci, J. W.; Kobayashi, Y.; Choi, G.; Alexandrescu, A. T.; Cole, J. L. Mechanism of Interaction of the Double-Stranded RNA (dsRNA) Binding Domain of Protein Kinase R with Short dsRNA Sequences. *Biochemistry* **2007**, *46*, 55−65.

(11) Cole, J. Activation of PKR: an open and shut case? *Trends Biochem. Sci.* **2007**, *32*, 57−62.

(12) Dey, M.; Cao, C.; Dar, A. C.; Tamura, T.; Ozato, K.; Sicheri, F.; Dever, T. E. Mechanistic Link between PKR Dimerization, Autophosphorylation, and eIF2α Substrate Recognition. *Cell* **2005**, *122*, 901−913.

(13) Lemaire, P. A.; Lary, J.; Cole, J. L. Mechanism of PKR activation: Dimerization and kinase activation in the absence of double-stranded RNA. *J. Mol. Biol.* **2005**, *345*, 81−90.

(14) Lemaire, P. A.; Anderson, E.; Lary, J.; Cole, J. L. Mechanism of PKR Activation by dsRNA. *J. Mol. Biol.* **2008**, *381*, 351−360.

(15) Husain, B.; Hesler, S.; Cole, J. L. Regulation of PKR by RNA: Formation of active and inactive dimers. *Biochemistry* **2015**, *54*, 6663−6672.

(16) Zerbe, C. M.; Cole, J. L. Regulation of Protein Kinase R by Epstein-Barr Virus EBER1 RNA. *Biochemistry* **2020**, *59*, 1252−1260.

(17) Spanggord, R. J.; Vuyisich, M.; Beal, P. A. Identification of binding sites for both dsRBMs of PKR on kinase-activating and kinase-inhibiting RNA ligands. *Biochemistry* **2002**, *41*, 4511−4520.

(18) Gelev, V.; Aktas, H.; Marintchev, A.; Ito, T.; Frueh, D.; Hemond, M.; Rovnyak, D.; Debus, M.; Hyberts, S.; Usheva, A.; Halperin, J.; Wagner, G. Mapping of the Auto-inhibitory Interactions of Protein Kinase R by Nuclear Magnetic Resonance. *J. Mol. Biol.* **2006**, *364*, 352−363.

(19) Nanduri, S.; Rahman, F.; Williams, B. R. G.; Qin, J. A dynamically tuned double-stranded RNA binding mechanism for the activation of antiviral kinase PKR. *EMBO J.* **2000**, *19*, 5567−5574.

(20) Ryter, J. M.; Schultz, S. C. Molecular basis of double-stranded RNA-protein interactions: structure of a dsRNA-binding domain complexed with dsRNA. *EMBO J.* **1998**, *17*, 7505−7513.

(21) Patel, R. C.; Stanton, P.; Sen, G. C. Specific Mutations Near the Amino Terminus of Double-stranded RNA-dependent Protein Kinase

(PKR) Differentially Affect Its Double-stranded RNA Binding and Dimerization Properties. *J. Biol. Chem.* **1996**, *271*, 25657−25663.
(22) Masliah, G.; Barraud, P.; Allain, F. H. RNA recognition by double-stranded RNA binding domains: A matter of shape and sequence. *Cell. Mol. Life Sci.* **2013**, *70*, 1875−1895.
(23) Stefl, R.; Oberstrass, F. C.; Hood, J. L.; Jourdan, M.; Zimmermann, M.; Skrisovska, L.; Maris, C.; Peng, L.; Hofr, C.; Emeson, R. B.; Allain, F. H.-T. The Solution Structure of the ADAR2 dsRBM-RNA Complex Reveals a Sequence-Specific Readout of the Minor Groove. *Cell* **2010**, *143*, 225−237.
(24) Husain, B.; Mukerji, I.; Cole, J. L. Analysis of high-affinity binding of protein kinase R to double-stranded RNA. *Biochemistry* **2012**, *51*, 8764−8770.
(25) Anderson, E.; Cole, J. L. Domain stabilities in protein kinase R (PKR): Evidence for weak interdomain interactions. *Biochemistry* **2008**, *47*, 4887−4897.
(26) VanOudenhove, J.; Anderson, E.; Krueger, S.; Cole, J. L. Analysis of PKR structure by small-angle scattering. *J. Mol. Biol.* **2009**, *387*, 910−920.
(27) Gleghorn, M. L.; Maquat, L. E. "Black sheep" that don't leave the double-stranded RNA-binding domain fold. *Trends Biochem. Sci.* **2014**, *39*, 328−340.
(28) Lemaire, P. A.; Tessmer, I.; Craig, R.; Erie, D. A.; Cole, J. L. Unactivated PKR exists in an open conformation capable of binding nucleotides. *Biochemistry* **2006**, *45*, 9074−9084.
(29) Peters, G. A.; Hartmann, R.; Qin, J.; Sen, G. C. Modular Structure of PACT: Distinct Domains for Binding and Activating PKR. *Mol. Cell. Biol.* **2001**, *21*, 1908−1920.
(30) Huang, X.; Hutchins, B.; Patel, R. C. The C-terminal, third conserved motif of the protein activator PACT plays an essential role in the activation of double-stranded-RNA-dependent protein kinase (PKR). *Biochem. J.* **2002**, *366*, 175−186.
(31) Li, S.; Peters, G. A.; Ding, K.; Zhang, X.; Qin, J.; Sen, G. C. Molecular basis for PKR activation by PACT or dsRNA. *Proc. Natl. Acad. Sci. U.S.A.* **2006**, *103*, 10005−10010.
(32) Maia de Oliveira, T.; Korboukh, V.; Caswell, S.; Winter Holt, J. J.; Lamb, M.; Hird, A. W.; Overman, R. The structure of human GCN2 reveals a parallel, back-to-back kinase dimer with a plastic DFG activation loop motif. *Biochem. J.* **2020**, *477*, 275−284.
(33) Padyana, A. K.; Qiu, H.; Roll-Mecak, A.; Hinnebusch, A. G.; Burley, S. K. Structural basis for autoinhibition and mutational activation of eukaryotic initiation factor 2alpha protein kinase GCN2. *J. Biol. Chem.* **2005**, *280*, 29289−29299.
(34) Anderson, E.; Pierre-Louis, W. S.; Wong, C. J.; Lary, J. W.; Cole, J. L. Heparin activates PKR by inducing dimerization. *J. Mol. Biol.* **2011**, *413*, 973−984.
(35) Ucci, J. W.; Cole, J. L. Global analysis of non-specific protein-nucleic interactions by sedimentation equilibrium. *Biophys. Chem.* **2004**, *108*, 127−140.
(36) Mayo, C. B.; Cole, J. L. Interaction of PKR with single-stranded RNA. *Sci. Rep.* **2017**, *7*, 3335.
(37) Wong, C. J.; Launer-Felty, K.; Cole, J. L. Analysis of PKR-RNA interactions by sedimentation velocity. *Methods Enzymol.* **2011**, *488*, 59−79.
(38) Stafford, W. F.; Sherwood, P. J. Analysis of heterologous interacting systems by sedimentation velocity: Curve fitting algorithms for estimation of sedimentation coefficients, equilibrium and kinetic constants. *Biophys. Chem.* **2003**, *108*, 231−243.
(39) Laue, T. M.; Shah, B. D.; Ridgeway, T. M.; Pelletier, S. L. Computer-aided interpretation of analytical sedimentation data for proteins. In *Analytical Ultracentrifugation in Biochemistry and Polymer Science*; Harding, S. E.; Rowe, A. J.; Horton, J. C., Eds.; Royal Society of Chemistry: Cambridge, U.K.., 1992; pp.90−125.

https://doi.org/10.1021/acsomega.1c00343
ACS Omega 2021, 6, 11367−11374